EXPLORATORY ‘OMIC ANALYSES ON THE EFFECTS OF COMBUSTIBLE AND ELECTRONIC CIGARETTE SMOKE

By

Matine Afari Rubin

A capstone project submitted for Graduation with University Honors

May 06, 2022

University Honors
University of California, Riverside

APPROVED

Dr. Prue Talbot
Department of Cell, Molecular, and Systems Biology

Dr. Richard Cardullo, Howard H Hays Jr. Chair
University Honors

1. ABSTRACT

There are an estimated 34.1 million cigarette smokers in the United States, with more than 16 million of those smokers living with smoking-related disease. In recent years, electronic cigarettes (e-cigarettes) have been gaining popularity as a safer, tobacco-free replacement to combustible tobacco cigarettes. While using e-cigarettes, or "vaping", is purportedly less harmful than smoking traditional tobacco products, it is not entirely safe due to the nicotine and chemical flavoring agents that are found in the e-cigarette liquid (e-liquid). As a result, the growing popularity of e-cigarettes has caused many users to experience detrimental e-cigarette, or vaping, product use associated lung injury (EVALI), contributing to the severity of e-cigarette use as a public health issue. Previous research has demonstrated possible adverse effects of smoking and vaping on a cellular level, but there is an absence of research regarding their effects on biological pathways in a systems-level approach. In this research project, I took an 'omics approach to addressing this topic by analyzing gene and protein expression changes due to exposure to cigarette smoke, e-cigarette aerosol, or e-liquid. By conducting comparative transcriptomics via RNA-Sequencing in human subjects and proteomics in tissue cultures that have been exposed to either combustible cigarette or e-cigarette aerosol, I contributed to a comprehensive understanding of the risks associated with using these smoking products. I hypothesize that many biological pathways will be significantly affected by smoke, aerosol, or e-liquid exposure, specifically those associated with cellular function, immune and inflammatory activity, and other diseases. This would provide strong evidence to suggest that e-cigarettes are not as safe as they were previously thought to be. Specifically, the purpose of the RNA-Seq. experiment was to show that e-cigarettes are not less harmful than traditional cigarettes, and that smokers who switch to e-cigarettes to quit smoking are still being exposed to harmful toxins. The purpose of

the proteomics experiment was to analyze the effects of thirdhand smoke (THS), the result of aged cigarette smoke, on human tissue cultures. The data and results discussed in this capstone project were written into two manuscripts, both of which are in review (see "Abstract References" section).

2. ACKNOWLEDGEMENTS

Although research projects that involve human subjects typically require approval by organizations such as the Institutional Review Boards (IRBs), the data that I analyzed was gathered before I became involved in the projects. The researchers who collected this data had previously obtained approval from the IRB to conduct their experiments with human subjects. I did not personally conduct any research involving human subjects; therefore, I did not need to apply for further approval by any review boards. The data analysis that I conducted does not require IRB approval.

I used QIAGEN's IPA software to analyze my data. An IPA license was obtained by Dr. Talbot for use by the laboratory and I had access to the software through TeamViewer. To ensure that I properly analyzed my 'omics datasets with IPA, I attended training webinars hosted by QIAGEN's scientists and researchers who specialize in data analysis with IPA. Additionally, I utilized prerecorded video tutorials that have been uploaded to the QIAGEN website to supplement the knowledge that I gained from the webinars to guarantee significant and accurate results.

I would like to thank Dr. Talbot, Giovanna Pozuelos, the graduate students from Dr. Talbot's laboratory, and their collaborators for conducting the primary research that produced the data I used for these 'omic investigations. I would also like to thank Dr. Talbot for her continued mentorship throughout the course of this project.

TABLE OF CONTENTS

3. INTRODUCTION AND BACKGROUND

Although cigarette smoking is on the decline among adults in the United States, nearly 40 million American adults continue to smoke cigarettes (CDCTobaccoFree, 2022). Although consistent cigarette use has the potential to cause severe smoking-related diseases, they are very hard to stop using due to their high nicotine content (Health, 2020; Kalkhoran & Glantz, 2016). Those who do attempt to quit find that smoking cessation is extremely difficult, causing the smoker to turn to nicotine replacement methods such as substituting the nicotine from combustible tobacco cigarettes with the heated, aerosolized nicotine found in e-cigarettes (CDC, 2020; Health, 2020; Hughes, 2003; Kalkhoran & Glantz, 2016). However, e-cigarettes have not been approved by the U.S. Food and Drug Administration (FDA) as safe or effective tools to quit smoking (CDC, 2020). Furthermore, individuals who successfully utilize e-cigarettes as an aid to quit smoking have a higher rate of continued use compared to other pharmacotherapy or nicotine replacement methods (Teriba et al., 2021). The nicotine from e-cigarettes can be addictive and there is no available pharmacotherapy intervention for the cessation of e-cigarettes use, meaning that users find it very difficult to quit using e-cigarettes, ultimately leading to long-term use (Teriba et al., 2021). Exposure to the nicotine found in e-liquid and e-cigarette aerosol can occur through inhalation, ingestion, and/or dermal contact. Although some research has been conducted to study the effects of dermal nicotine uptake during the harvesting of tobacco leaves (McKnight & Spiller, 2005), little is known about the effects of dermal nicotine exposure caused by contact with e-liquid. THS is another environmental contaminant that causes dermal nicotine uptake. The main constituent of THS is nicotine, along with other carcinogenic chemicals (Bahl et al., 2016; Pozuelos et al., 2021).

Since their popularization in the early 2010's, e-cigarettes have been commonly believed to be a safer alternative to cigarettes because they are able to deliver nicotine to the smoker by heating the e-liquid rather than burning tobacco (Canistro et al., 2017; CDC, 2020; Health, 2020). Although e-cigarettes do contain less harmful chemicals than traditional combustible cigarettes, the liquid aerosolization process that occurs in e-cigarettes heats the nicotine and flavoring-containing liquid to >200 degree Celsius, which generates toxic and carcinogenic substances within the device that are inhaled by the user (Canistro et al., 2017). Furthermore, e-cigarettes have been reported to cause e-cigarette, or vaping, product use associated lung injury (EVALI) (Salzman et al., 2019). The EVALI epidemic began in 2019, wherein over 2,000 cases of EVALI were reported as of November 2019 (Salzman et al., 2019). Those affected by EVALI suffer severe lung injury as a result of e-cigarette use, suggesting that e-cigarette use has the potential to be detrimental to one's health, if not fatal (Salzman et al., 2019). As of February 2020, the Center for Disease Control (CDC) reported that just under 3,000 instances of EVALI resulted in hospitalization in the United States, while 68 of those resulted in death (McAlinden et al., 2020).

Recent scientific studies have called into question the safety of e-cigarettes by utilizing animal and *in vitro* cell culture models. One study found that e-cigarette exposure in a rat lung model caused an increase in phase I carcinogen-bioactivating enzymes, polycyclic aromatic hydrocarbons (PAHs), oxygen free-radical production, and DNA damage observed from the chromosomal level to the gene level (e.g. point mutations, etc.) (Canistro et al., 2017). These toxicological effects are known to increase the risk of cancer, indicating that e-cigarettes could be carcinogenic much like combustible cigarettes (Singh et al., 2016). Another study utilized human pulmonary fibroblasts, lung epithelial cells, and human embryonic stem cells to assess

cellular response to e-cigarette liquids and aerosols, ultimately demonstrating that exposure induced cytotoxic effects (Behar et al., 2018). To gain a better understanding of these carcinogenic and cytotoxic effects of continued e-cigarette use, further studies involving human subjects and human tissue cultures are necessary. The experiments described in my capstone aim to address these gaps in the research by analyzing the effects of e-cigarettes, nicotine, and/or THS.

Thirdhand smoke (THS), the tobacco residue that is left behind after secondhand smoke has settled onto surfaces (Jacob et al., 2017), is another contaminant of interest. THS is characterized by the "four Rs," meaning the potentially toxic chemicals caused by smoking must have remained, reacted, re-emitted, and/or resuspended after the smoking event has ended (Jacob et al., 2017). THS poses its own unique threat to human health because it has been shown that cigarette aerosol becomes more toxic as it remains on a surface for some time after exhalation (Jacob et al., 2017). Namely, increased concentrations of carcinogenic tobacco-specific nitrosamines (TSNAs) is observed in aged tobacco aerosol, caused by the nicotine within the aerosol interacting with pollutants found indoors (Sleiman et al., 2010). These common conditions indicate that exposure to known toxins found in THS is highly likely, either through inhalation, dermal exposure, or both (Jacob et al., 2017). Given that nicotine is one of the main substituents of THS, dermal exposure to THS was experimentally modeled in Section 5.1 by treating EpiDerm™, a 3D human tissue culture, with different concentrations of nicotine.

Dermal exposure to and uptake of nicotine from both e-liquid and THS can occur in many ways in adults and children alike. These substances may come into contact with skin if contaminated household or public surfaces are touched, or even if contaminated clothes are worn (Matt et al., 2011; Pozuelos et al., 2021). Cotinine, which is a nicotine metabolite that indicates

exposure to the chemical, was detected in the urine and hair of children who lived with parents who smoked (Matt et al., 2004), indicating that nicotine is readily absorbed by the human body upon exposure to THS. Dermal exposure to the nicotine in e-liquid has also been observed. E-cigarette users may dermally contact e-liquid during use if the fluid leaks from the device itself or if surfaces contaminated with the fluid or residue are touched (Garcia et al., 2016; Khachatoorian et al., 2019). While one study found that levels of nicotine in THS vary from ~10 $\mu g/m^2$ to ~70 $\mu g/m^2$ (Matt et al., 2004), it was determined that e-liquid contain very high concentrations of nicotine, ranging from 1-100 mg/mL (Davis et al., 2015). The EpiDerm™ samples involved in the experiment described in Section 5.1 were exposed to two levels of nicotine, either 10 μg/mL or 400 μg/mL, to model the realistic levels of nicotine that are observed outside of controlled research conditions.

My Capstone project aimed to investigate the effects of chronic e-cigarette exposure in humans and acute nicotine exposure in tissue culture samples through 'omic analyses. I analyzed RNA-Seq./transcriptomic and proteomic data from previously conducted experiments to assess the expression and regulatory changes of significantly affected genes and proteins. This analysis aimed to provide a comprehensive look at the effects of these relevant chemicals by exploring biological pathways that were activated or suppressed throughout the body. By conducting my project with this approach, I reported comprehensive results from multiple levels of molecular data. Analyzing more than one 'omic dataset provided better insight into the affected biological systems, compared to a singular dataset analysis (Subramanian et al., 2020). A limitation of past studies that I addressed in my Capstone project is the lack of contextualized results. I maintained a systems-level approach to biological pathway analysis which ensured that a given result was understood within the context of larger systems at work within the experimental model (Draghici

et al., 2007). Along with common statistical results, this systems-level analysis also took into account the magnitude of expression change, position of the molecule within the biological pathway, and the term's interactions with other molecules (Draghici et al., 2007). With this project, I contributed to the growing body of knowledge on the risks of e-cigarette and THS exposure. The first experiment discussed in Section 4.1 utilized RNA-Seq. methods to investigate whether participants who switched from combustible cigarettes to e-cigarettes experienced a reduction of harmful. This research will help determine if switching to e-cigarettes is healthier than continued combustible cigarette use. The second experiment discussed in Section 5.1 analyzed proteomic data from human 3D skin cultures that were exposed to varying levels of nicotine to understand how dermal exposure to these chemicals affect protein expression.

4. GENERAL METHODS

4.1 Ingenuity Pathway Analysis (IPA)

IPA software (QIAGEN Inc., https://digitalinsights.qiagen.com/IPA) was used to analyze both sets of data from the experiments described in Sections 4.1 and 5.1 IPA is a biological pathway analysis software powered by the Ingenuity Knowledge Base that allows significant Diseases and Biological Functions, Canonical Pathways, and Regulator Effects to be identified. The Ingenuity Knowledge Base is a manually curated collection of millions of published biomedical findings that allows IPA to verify datasets that are uploaded into the software (Krämer et al., 2014). Significant Diseases and Biological Functions were identified using the right-tailed Fisher's exact test and associated p-value. The top Canonical Pathways were ranked by z-score produced with IPA's algorithm. Regulator Effects were investigated to identify upstream regulators and associated biological processes found to be affected within the data.

Prior to the core analysis of the RNA-Seq. data, “human” and “lung system” prefilters were applied. The “human” prefilter was more general and allowed information about any human biological pathway to be included in the analysis. The “lung system” prefilter allowed for a more specified analysis by excluding non-lung related information ahead of analysis. The following cutoff values were applied to the data: log-fold change +/-0.6, p-value 0.05, and q-value 0.05.

4.2 Disease Ontology Semantic and Enrichment (DOSE)

In addition to IPA, DOSE was implemented to identify similarities among disease ontology (DO) terms and known genes. DOSE was developed within the R statistical computing environment and released under the Bioconductor project. Enrichment gene set analysis was conducted using DOSE to discover disease associations within the biological data gathered from the experiments described in Sections 4.1 and 5.1 (Yu et al., 2015). Significant associations between differentially expressed genes (DEGs) and DO terms were identified using hypergeometric testing. The *cnetplot* function in R was utilized to provide a visualization of the significant DEG-disease association networks.

5. RNA-SEQUENCING/TRANSCRIPTOMICS ANALYSIS

5.1 Specific Methods

Data for this transcriptomic analysis was collected by a former post-doctorate student from Dr. Talbot’s laboratory. Nasal epithelium biopsies from 22 human participants were collected and shipped frozen to the University of California, Riverside (UCR) where they remained until RNA extraction was performed. RNA samples were extracted at UCR and shipped on dry ice to Cofactor Genomics in St. Louis, MO where the RNA library was prepared, sequenced, and checked for quality.

Nasal epithelium biopsy samples from 19 female participants were selected to undergo RNA-Seq. analysis. This selection was determined by gender, age, ethnicity, urine cotinine concentrations, and RNA quality. Urine cotinine levels and information on smoking history were collected at the time of biopsy sampling and used to verify whether the participant was a non-smoker (NS) or not. Those included in the NS (control) group were verified with a urine cotinine measurement of 0 ng/mL. The experimental groups were classified as those who were cigarette users (CS), or those who were previous cigarette users and had switched to using e-cigarettes as a complete replacement for cigarettes for at least 6 months (EC). The inclusion of participants in the CS and EC groups was validated with urine cotinine levels of at least 400 ng/mL.

The FASTQ files containing the sequenced RNA base pairs were processed at the University of California. The data were preprocessed before differential expression analysis to remove low-quality datapoints. Then, the sequenced RNA within the FASTQ files were aligned to the Human reference genome (UCSC hg19) acquired from Illumina iGenomes (ftp.illumina.com). Hierarchical clustering was conducted using Spearman's correlation values to identify outliers in each of the comparison groups: EC vs NS, CS vs NS, and CS vs EC. After outliers were removed, differential gene expression analysis was performed between the three comparison groups as well. At the end of this process, each comparison group contained the data from three participants. Information on the demographics, smoking history, and biomarker data of the included participants can be found in Table 1.

Sample Name	Age	Group	Smoking History	Cigs/Day	Puffs/Day	E-cig Nicotine Concentration	Brand	Current Flavor	Urine Cotinine Concentration (ng/mL)
72	29	E-cigarette			90	6-9 mg (0.6-0.9%)	Smoov		1021.15457
132	32	E-cigarette			96	16-24 mg (1.6-2.4%)	Smoov		711.214864
188	39	E-cigarette			100	6-9 mg (0.6-0.9%)	ECTO		478.253462
75	48	Non-smoker	Never smoker						0
183	38	Non-smoker	Ex-smoker						0
254	26	Non-smoker	N/A						N/A
40	33	Smoker		1					927.192474
85	33	Smoker		12					920.036049
98	41	Smoker		24					1103.99238

Table 1: Demographics and Biomarker Data. This Table was created by another researcher during preliminary data analysis.

5.2 Results

An FDR cut-off value of 0.05 or less and an absolute log2-fold change of 1 or greater were used to identify significant DEGs. Figure 1A summarizes overlapping overall DEGs between the three comparison groups (EC vs. NS, CS vs. NS, and CS vs. EC). EC vs. NS and CS vs. NS had the greatest number of overlapping DEGs with a count of 280 (Figure 1A). Figure 1B shows the up and downregulated DEGs for the three comparison groups. Downregulated EC vs. NS and downregulated CS vs. NS had the greatest number of overlapping DEGs with a count of 197 (Figure 1B).

A.

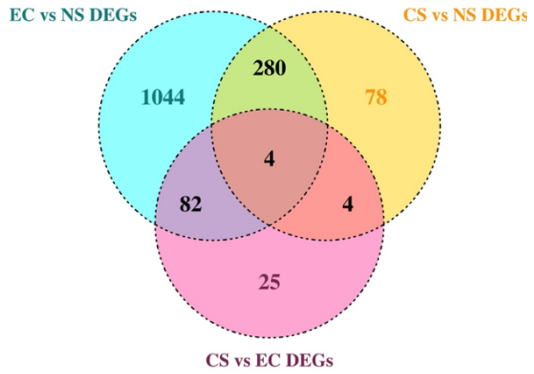

B.

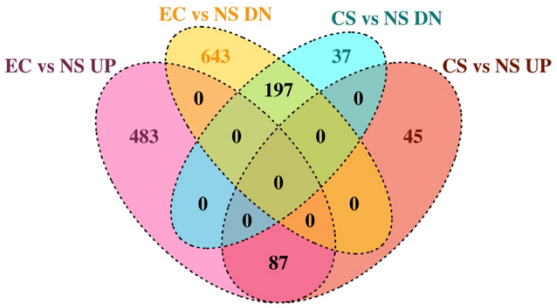

Figure 1: (A) Venn diagram depicting all DEGs in the three comparison groups. (B) Venn diagram comparing up and downregulated DEGS (FDR < 0.05) in EC vs. NS and CS vs. NS. These figures were created by another researcher during early stages of analysis.

Gene ontology (GO) term enrichment analysis was performed to identify over-represented DEGs using ClusterProfiler in R/Bioconductor. The over-represented DEGs correspond with affected biological processes in each group, shown in Figure 2. These pathways and GO terms were determined with a cut-off adjusted p-value of 0.05 using the Bonferroni Hochberg statistical analysis. The top enriched biological process categories for the downregulated DEGs in the EC vs. NS comparison group were mostly related to ciliary health and included terms such as cell projection assembly, plasma membrane bounded cell projection assembly, cilium organization, microtubule-based movement, and microtubule cytoskeleton organization (Figure 2A). Other top biological processes identified by downregulated genes in this comparison group included nervous system process, pattern specific process, regulation of ion transport, and monovalent inorganic cation transport (Figure 2A).

The enriched biological processes that were identified by upregulated DEGs in EC vs. NS comparison group were largely related to immune and inflammatory responses and included myeloid leukocyte mediated immunity, leukocyte degranulation, neutrophil activation, granulocyte activation, neutrophil degranulation, neutrophil activation involved in immune

response, neutrophil mediated immunity, and inflammatory response (Figure 2B). Other top processes included response to wounding and epithelial cell differentiation, and were both related to dermal health (Figure 2B).

In the CS vs. NS comparison group, the affected biological processes identified by the downregulated DEGs were similar to the cilia-related processes observed in the downregulated EC vs. NS group. The specific processes were microtubule-based movement, plasma membrane bounded cell projection assembly, cell projection assembly, cilium assembly, cilium organization, cilium movement, cilium or flagellum-dependent cell motility, and cilium-dependent cell motility (Figure 2C). Compared to the processes from the EC vs. NS downregulated DEGs, these terms focused more on cell motility in relation to cilia health.

The upregulated DEGs in the CS vs. NS comparison group were used to identify the following affected biological processes: monocarboxylic acid metabolic process, anion transport, retinoid metabolic process, diterpenoid metabolic process, terpenoid metabolic process, isoprenoid metabolic process, cellular response to xenobiotic stimulus, regulation of hormone levels, and organic anion transport (Figure 2D). These processes were mostly related to metabolic processes.

The top affected biological processes for downregulated CS vs. EC genes were mainly related to immune and inflammatory responses and included terms such as neutrophil activation, granulocyte activation, neutrophil degranulation, neutrophil activation involved in immune response, neutrophil mediated immunity, leukocyte degranulation, myeloid cell activation involved in immune response, myeloid leukocyte mediated immunity, and inflammatory response (Figure 2E). The one other top affected process not related to immune and inflammatory response was epidermis development (Figure 2E).

In the CS vs. EC comparison group, the top biological processes identified with upregulated DEGs were mostly related to cilia health and included cilium assembly, cilium organization, plasma membrane bounded cell projection assembly, cell projection assembly, microtubule-based movement, cilium movement, axoneme assembly, and microtubule bundle formation (Figure 2E). Other processes included determination of left/right symmetry and determination of bilateral symmetry (Figure 2E).

A.

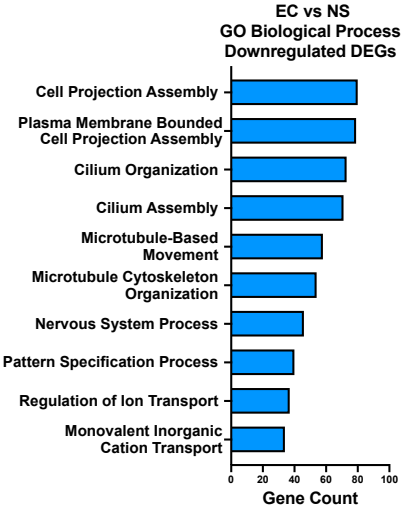
EC vs NS
GO Biological Process
Downregulated DEGs
Cell Projection Assembly
Plasma Membrane Bounded Cell Projection Assembly
Cilium Organization
Cilium Assembly
Microtubule-Based Movement
Microtubule Cytoskeleton Organization
Nervous System Process
Pattern Specification Process
Regulation of Ion Transport
Monovalent Inorganic Cation Transport
0 20 40 60 80 100
Gene Count

B.

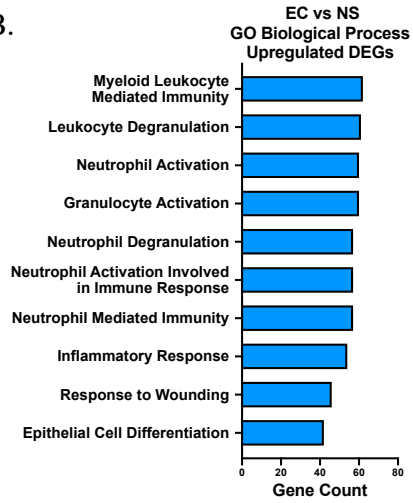
EC vs NS
GO Biological Process
Upregulated DEGs
Myeloid Leukocyte Mediated Immunity
Leukocyte Degranulation
Neutrophil Activation
Granulocyte Activation
Neutrophil Degranulation
Neutrophil Activation Involved in Immune Response
Neutrophil Mediated Immunity
Inflammatory Response
Response to Wounding
Epithelial Cell Differentiation
0 20 40 60 80
Gene Count

C.

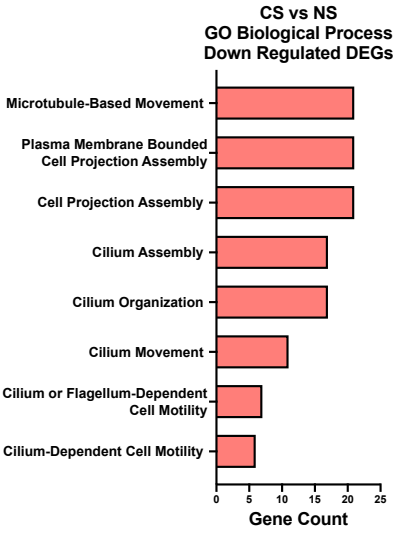
CS vs NS
GO Biological Process
Down Regulated DEGs
Microtubule-Based Movement
Plasma Membrane Bounded Cell Projection Assembly
Cell Projection Assembly
Cilium Assembly
Cilium Organization
Cilium Movement
Cilium or Flagellum-Dependent Cell Motility
Cilium-Dependent Cell Motility
0 5 10 15 20 25
Gene Count

D.

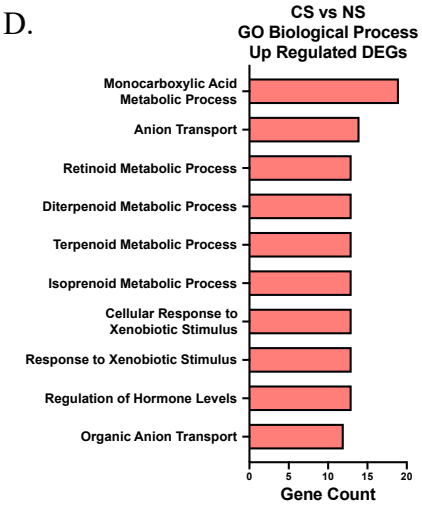
CS vs NS
GO Biological Process
Up Regulated DEGs
Monocarboxylic Acid Metabolic Process
Anion Transport
Retinoid Metabolic Process
Diterpenoid Metabolic Process
Terpenoid Metabolic Process
Isoprenoid Metabolic Process
Cellular Response to Xenobiotic Stimulus
Response to Xenobiotic Stimulus
Regulation of Hormone Levels
Organic Anion Transport
0 5 10 15 20
Gene Count

E.

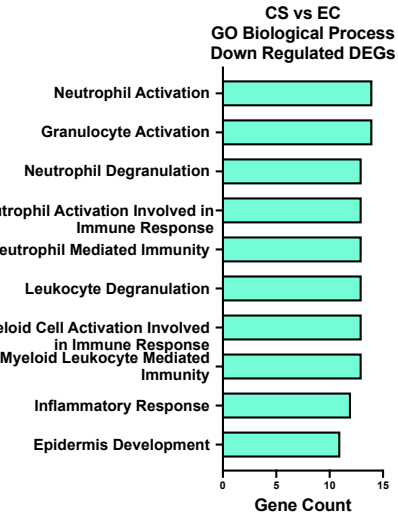
CS vs EC
GO Biological Process
Down Regulated DEGs
Neutrophil Activation
Granulocyte Activation
Neutrophil Degranulation
Neutrophil Activation Involved in Immune Response
Neutrophil Mediated Immunity
Leukocyte Degranulation
Myeloid Cell Activation Involved in Immune Response
Myeloid Leukocyte Mediated Immunity
Inflammatory Response
Epidermis Development
0 5 10 15
Gene Count

F.

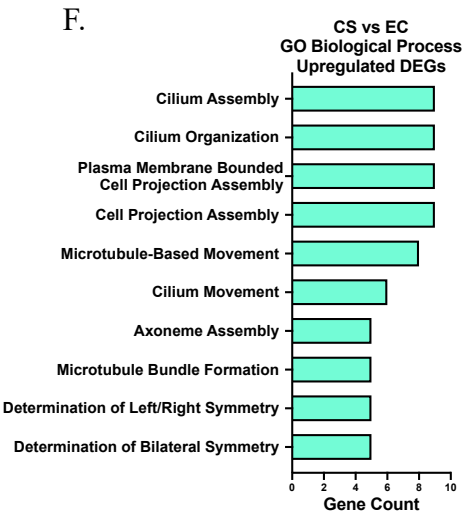
CS vs EC
GO Biological Process
Upregulated DEGs
Cilium Assembly
Cilium Organization
Plasma Membrane Bounded Cell Projection Assembly
Cell Projection Assembly
Microtubule-Based Movement
Cilium Movement
Axoneme Assembly
Microtubule Bundle Formation
Determination of Left/Right Symmetry
Determination of Bilateral Symmetry
0 2 4 6 8 10
Gene Count

Figure 2: Top 10 enriched GO term annotations for each of the three comparison groups. (A) Significantly enriched downregulated biological processes in EC vs. NS. (B) Significantly enriched upregulated biological processes in EC vs. NS. (C) Significantly enriched downregulated biological processes in CS vs. NS. (D) Significantly enriched upregulated biological processes in CS vs. NS. (E) Significantly enriched downregulated biological processes in CS vs. EC. (F) Significantly enriched downregulated biological processes in CS vs. EC. These figures were created by another researcher during early stages of.

IPA was used to analyze which diseases and biological functions were significantly affected (z-score ≥ 2 or ≤ -2) within the EC vs. NS comparison group. The DEGs were filtered using an IPA setting to only include lung-related genes. Disease and biological function analysis of the lung-filtered data from the EC vs. NS comparison group demonstrated an increase in functions related to inflammation and immune activation, such as response of myeloid cells and degranulation of phagocytes (Table 2). This analysis also determined that there was a decrease in formation of cilia within the same comparison group (Table 2). Other top increased diseases or biological functions were related to cell-to-cell signaling, cellular movement, cancer, and lipid metabolism (Table 2). There were no significantly affected diseases or biological functions in the other two comparison groups (CS vs. NS and CS vs. EC).

Categories	**Diseases or Functions Annotation**	**p-value**	**Predicted Activation State**	**Activation z-score**	**# Molecules**
Cell-to-Cell Signaling and Interaction	Response of myeloid cells	0.00744	Increased	2.95	19
Cellular Compromise, Inflammatory Response	Degranulation of myeloid cells	8.35E-06	Increased	2.8	63
Cellular Compromise, Inflammatory Response	Degranulation of phagocytes	5.29E-06	Increased	2.8	63
Cellular Movement, Hematological System Development and Function,	Homing of leukocytes	0.00737	Increased	2.735	34

Immune Cell Trafficking					
Cellular Movement	Cell movement	0.0001	Increased	2.615	218
Cancer, Organismal Injury and Abnormalities, Respiratory Disease	Lung cancer	0.000446	Increased	2.608	350
Cell-to-Cell Signaling and Interaction	Response of granulocytes	0.000255	Increased	2.538	12
Cancer, Organismal Injury and Abnormalities	Extraadrenal retroperitoneal tumor	0.000127	Increased	2.449	329
Cellular Compromise, Inflammatory Response	Degranulation of leukocytes	1.33E-05	Increased	2.395	64
Lipid Metabolism, Small Molecule Biochemistry	Conversion of eicosanoid	0.00309	Increased	2.372	6
Cell Morphology, Cellular Assembly and Organization, Cellular Function and Maintanence	Formation of cilia	1.61E-07	Decreased	-2.158	30

Table 2: Top Biological Functions for EC vs. NS using Human Lung-Filtered Data.

Disease ontology analysis was conducted using the DOSE package in R for the up and downregulated DEGs identified in the EC vs. NS comparison group. The top affected disease categories for the upregulated genes included cell surface interactions at the vascular wall, formation of the cornified envelope, interleukin-4 and interleukin-13 signaling, keratinization, and neutrophil degranulation (Figure 3). Most of the identified categories in this analysis were related to immune and inflammatory response, much like those identified by IPA. The CNET plot illustrating the results from this DOSE analysis showed that the DEGs associated with these various disease categories often overlapped and contributed to the upregulation of more than one disease (Figure 3).

Similarly, DOSE was used to analyze the downregulated DEGs from the EC vs. NS comparison group. The top affected disease categories for the downregulated genes included anchoring of the basal body to the plasma membrane, cilium assembly, hedgehog "off" state, intraflagellar transport, organelle biogenesis and maintenance, and signaling by hedgehog (Figure 4). Most of the identified categories in this analysis were related to cilia health, much like those identified by IPA. The CNET plot illustrating the results from this DOSE analysis showed that the DEGs associated with these various disease categories often overlapped and contributed to the downregulation of more than one disease (Figure 4).

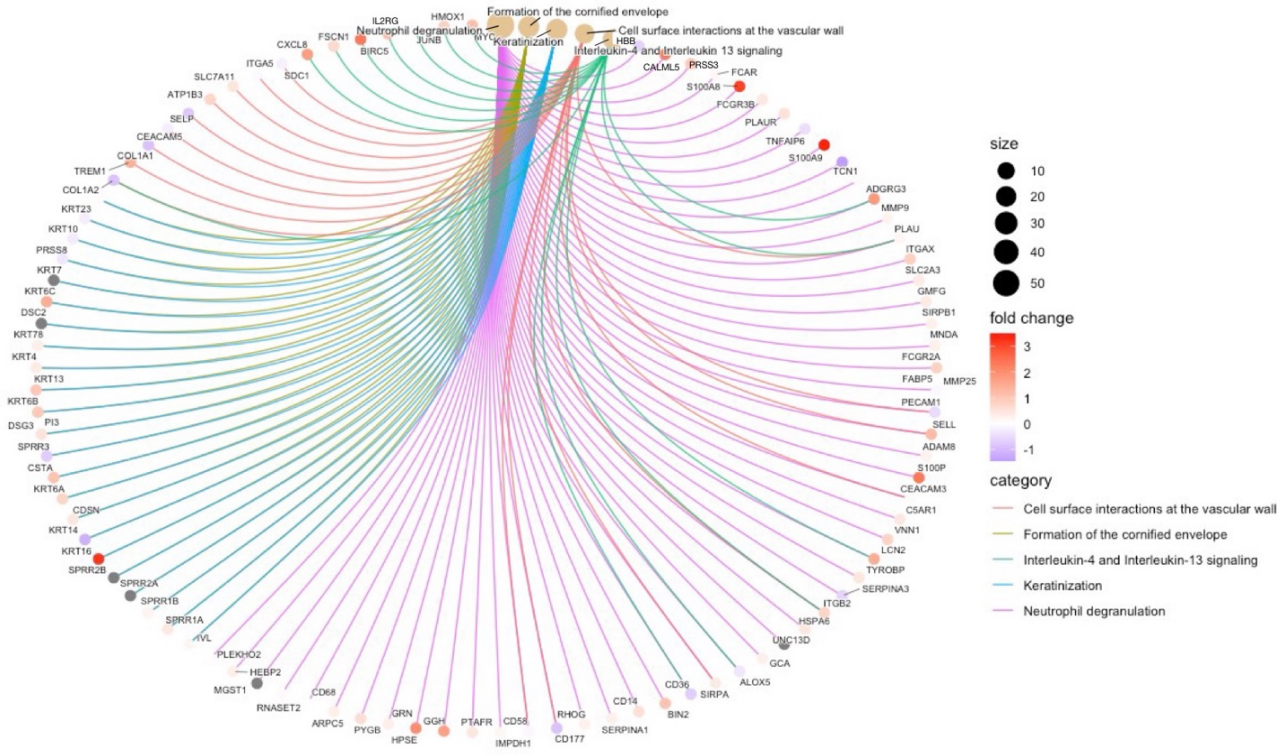

Figure 3: CNET Plot of Upregulated DEGs EC vs. NS. Plot shows the DEGs contributing to the upregulation of each identified disease. Circle size of disease node indicates number of genes associated with each disease.

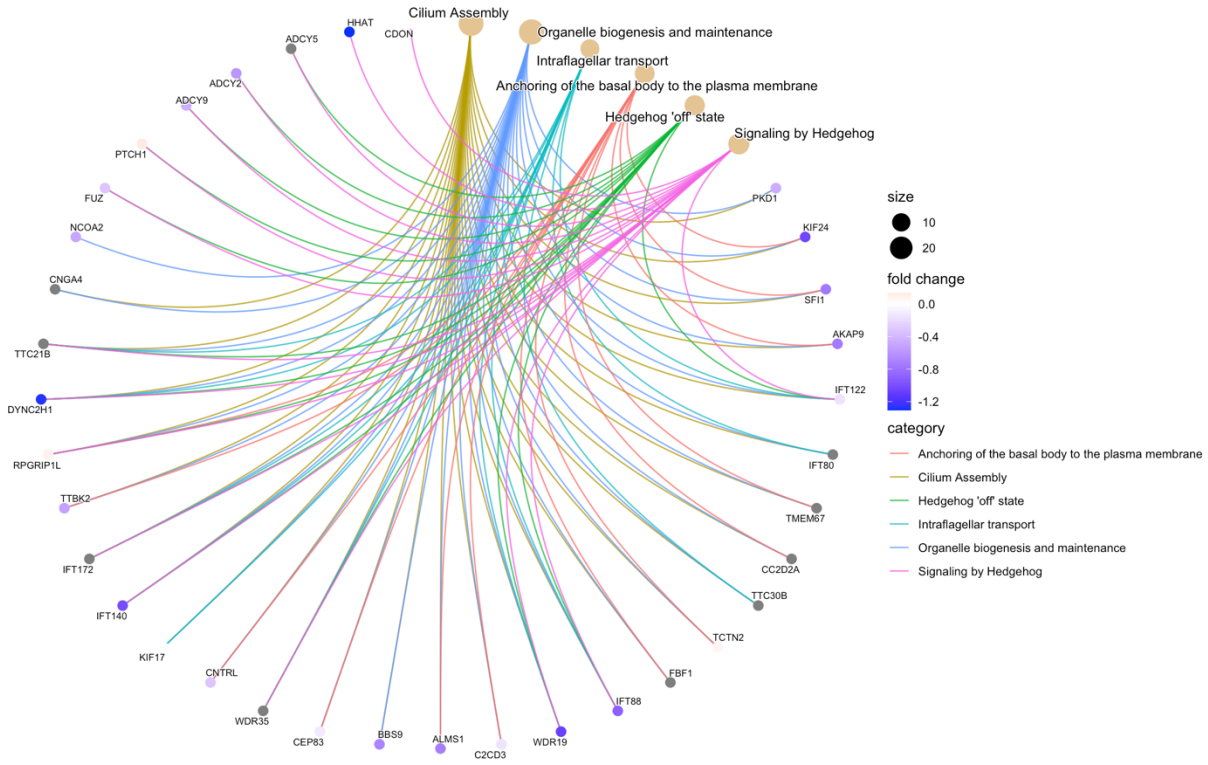

Figure 4: CNET Plot of Downregulated DEGs EC vs. NS. Plot shows the DEGs contributing to the downregulation of each identified disease. Circle size of disease node indicates number of genes associated with each disease.

IPA was also used to perform canonical pathway analysis for the lung-filtered DEGs in the three comparison groups. One significant canonical pathway was identified in the EC vs. NS group: leukocyte extravasation signaling (Table 3). No significant canonical pathways were identified in the CS vs. NS comparison group (Table 4). Several canonical pathways were identified to be significant in the CS vs. EC comparison. These included LXR/RXR activation, osteoarthritis pathway, and cardiac hypertrophy signaling (Table 5).

EC vs. NS		
Ingenuity Canonical Pathways	**-log(p-value)**	**z-score**
Inhibition of Matrix Metalloproteases	2.74E+00	-1.633
Granulation Adhesion and Diapedesis	2.68E+00	NaN
LPS/IL-1 Mediated Inhibition of RXR Function	2.40E+00	1.134
Oxidative Ethanol Degradation III	2.39E+00	0
Fatty Acid Activation	2.32E+00	0
Vitamin-C Transport	2.21E+00	0
Tryptophan Degradation X (Mammalian, via Tryptamine)	1.79E+00	0
Atherosclerosis Signaling	1.75E+00	NaN
γ-linolenate Biosynthesis II (Animals)	1.75E+00	0
Mitochondrial L-carnitine Shuttle Pathway	1.75E+00	0
Agranulocyte Adhesion and Diapedesis	1.69E+00	NaN
LXR/RXR Activation	1.64E+00	-1.508
Putrescine Degradation III	1.61E+00	0
Methylglyoxal Degradation III	1.60E+00	NaN
Estrogen Biosynthesis	1.58E+00	1.342
Melatonin Degradation II	1.56E+00	NaN
Acetate Conversion to Acetyl-CoA	1.56E+00	NaN
Dopamine Degradation	1.48E+00	0
Role of IL-17A in Psoriasis	1.43E+00	NaN
Ethanol Degradation IV	1.37E+00	0
Leukocyte Extravasation Signaling	1.30E+00	2.668

Table 3: Top Canonical Pathways for EC vs. NS using Human Lung-Filtered Data.

CS vs. NS		
Ingenuity Canonical Pathways	**-log(p-value)**	**z-score**
Tryptophan Degradation X (Mammalian, via Tryptamine)	2.33E+00	NaN
Methylglyoxal Degradation III	2.03E+00	NaN
Putrescine Degradation III	1.57E+00	NaN
Fatty Acid α-oxidation	1.57E+00	NaN
Inhibition of Matrix Metalloproteases	1.57E+00	NaN
Serotonin Degradation	1.53E+00	NaN
Dopamine Degradation	1.50E+00	NaN
Epoxysqualene Biosynthesis	1.36E+00	NaN

Table 4: Top Canonical Pathways for CS vs. NS using Human Lung-Filtered Data.

CS vs. EC		
Ingenuity Canonical Pathways	**-log(p-value)**	**z-score**
Granulocyte Adhesion and Diapedesis	5.50E+00	NaN
MSP-RON Signaling Pathway	4.40E+00	NaN
Agranulocyte Adhesion and Diapedesis	4.22E+00	NaN
Role of Macrophages, Fibroblasts and Endothelial Cells in Rheumatoid Arthritis	3.59E+00	NaN
Complement System	3.44E+00	NaN
LXR/RXR Activation	3.08E+00	2
Phagosome Formation	2.85E+00	NaN
Osteoarthritis Pathway	2.71E+00	-2
Cardiac Hypertrophy Signaling (Enhanced)	1.81E+00	-2

Table 5: Top Canonical Pathways for CS vs. EC using Human Lung-Filtered Data.

IPA's regulator effect analysis for the EC vs. NS comparison produced the top regulator effect network shown in Figure 5. This figure shows the five predicted upstream regulators and their connection to 12 DEGs identified in our data. Those DEGs were then linked to three downstream functions that were predicted to have been activated (Figure 5). These functions were all related to inflammatory and immune responses, and included inflammatory response, homing of leukocytes, and degranulation of cells (Figure 5).

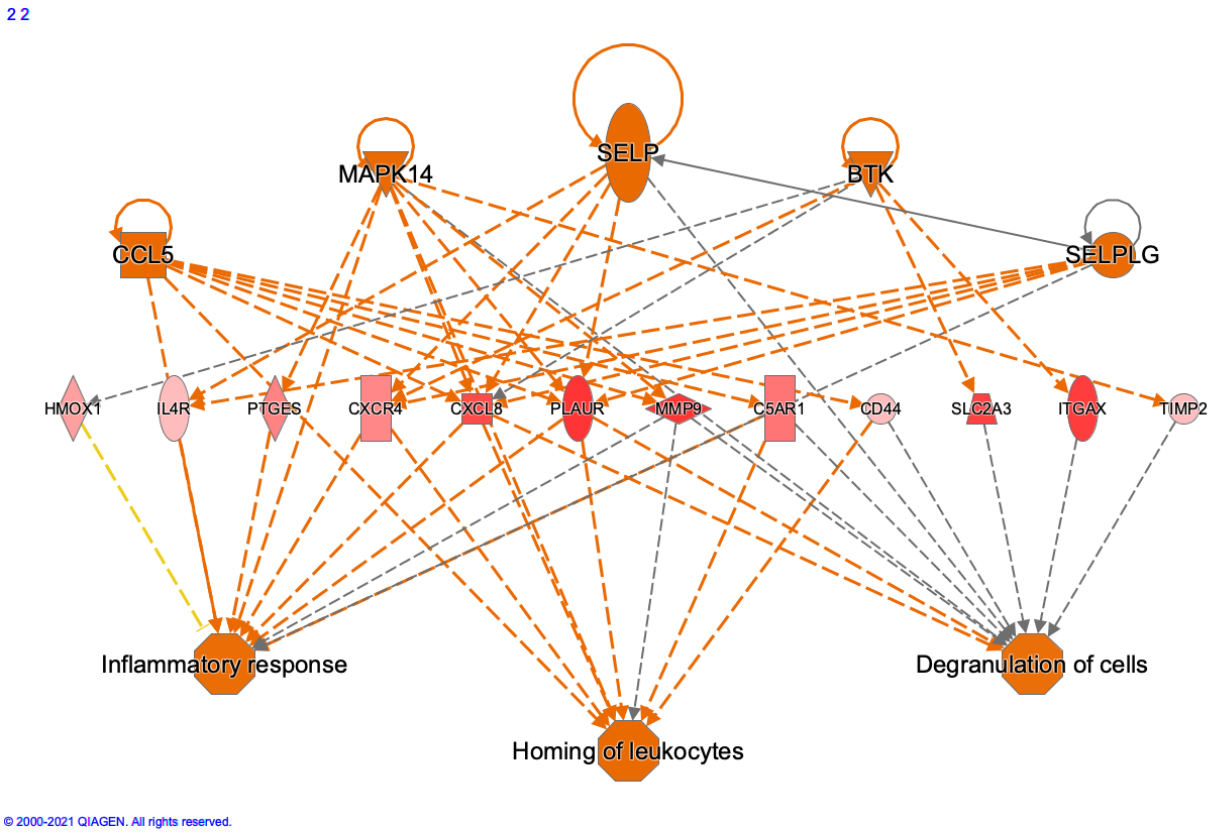

Figure 5: Regulator Effects for EC vs. NS using Human Lung-Filtered Data.

6. PROTEOMICS ANALYSIS

6.1 Specific Methods

The experiments to gather proteomic data were conducted by a former graduate student in Dr. Talbot's laboratory. This set of experiments utilized an *in vitro* 3D human skin model with EpiDerm™ (EPI-200) produced by Mat-Tek Corporation in Ashland, MA, USA. EpiDerm™ is a highly differentiated 3D model of human-derived epidermal keratinocytes. EpiDerm™ was cultured on tissue culture inserts with the air-liquid interface method to allow for the evaluation of exposure to applied chemicals and compounds.

Initially, the apical surface of the EpiDerm™ samples were treated with phosphate buffered saline (PBS) only, 10 µg/mL (Nic10), or 400 µg/mL (Nic400) liquid (-)-nicotine diluted in PBS. EpiDerm™ samples were treated for 24 hours and then lysed to begin preparing the

samples for proteomic analysis. After the EpiDerm^{TM} samples were treated with a digestion buffer, the protein material within the tissue culture was induced to bind to carboxylate-modified magnetic beads (CMMB). The CMMB were washed with ethanol and the resulting protein samples were further digested and resuspended to obtain eluted peptide samples. The peptide samples were then reconstituted in formic acid ahead of analysis by liquid chromatography with tandem mass spectrometry (LC-MS/MS). Sample analysis was conducted at the University of California, Los Angeles proteomics core.

The peptide samples were separated, and MS/MS spectra were obtained using the Data Dependent Acquisition (DDA) mode on a Thermo Orbitrap-Fusion Lumos Tribrid mass spectrometer. Data analysis of the MS/MS spectra was conducted using MaxQuant, a quantitative proteomic software, with a human proteome reference from EMBL (UP000005640_9606 HUMAN Homo sapiens, 20874 entries) for protein identification. Relative protein abundance quantification was performed and the data between biological replicates were compared and modified for quality. Significant proteins were identified with a corresponding p-value of 0.05or less and an absolute log-2-fold change of 0.1 or greater.

6.2 Results

Figure 6A summarizes overlapping overall differentially expressed proteins between the two comparison groups (Nic10 vs. PBS and Nic400 vs. PBS). Nic10 vs. PBS and Nic400 vs. PBS had 110 overlapping differentially expressed proteins (Figure 6A). Figure 6B shows the up and downregulated differentially expressed proteins for the two comparison groups. Downregulated Nic10 vs. PBS and downregulated Nic400 vs. PBS had 50 overlapping proteins while the upregulated comparison groups had 56 overlapping proteins (Figure 6B).

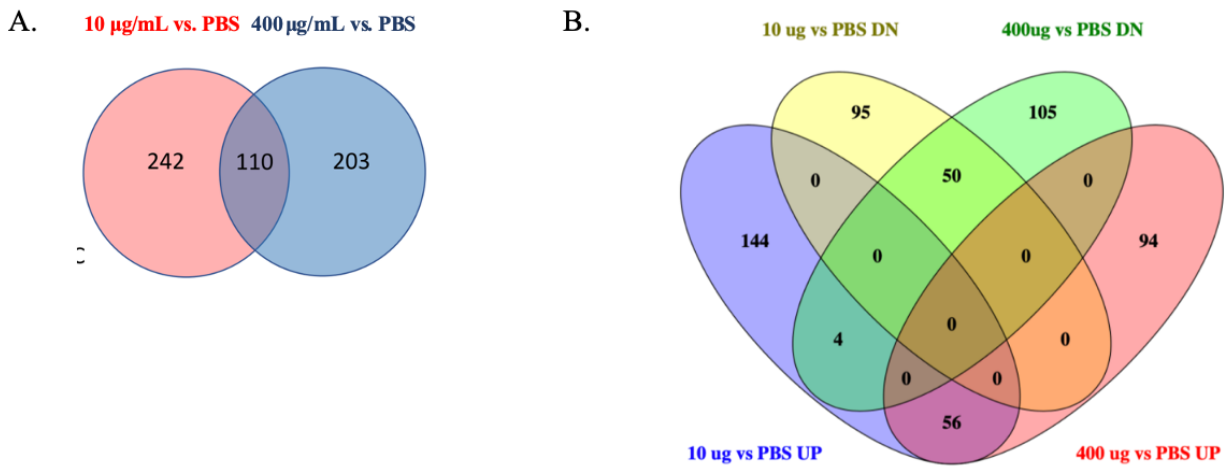

Figure 6: (A) Venn diagram depicting all differentially expressed proteins in the two comparison groups including number of overlapping proteins. (B) Venn diagram comparing up and downregulated differentially expressed proteins in 10 µg/mL vs. PBS and 400 µg/mL vs. PBS. These figures were created by another researcher during early stages of analysis.

Significant (z-score ≥ 2 or ≤ -2) canonical pathways identified within the Nic10 vs. PBS comparison group had either positive z-scores, indicating pathway activation, or negative z-scores, indicating pathway suppression. The significant pathway with a positive z-scores was EIF2 signaling (protein synthesis-related pathway) (Table 6). The significant pathway with a negative z-score was TNFR1 signaling (apoptosis-related pathway) (Table 6). Other pathways that were identified to have negative z-scores included immune and inflammatory-related pathways (Table 6). Specifically, these downregulated pathways were the role of MAPK signaling in promoting the pathogenesis of influenza, IL-6 signaling, IL-1 signaling, LPS-stimulated MAPK signaling, IL-15 production, and IL-8 signaling, which indicate anti-inflammatory response (Table 6). The Nic400 vs. PBS pathways with a positive z-score was also EIF2 signaling (protein synthesis-related pathway) (Table 7). There were no significant pathways with a negative z-score for this comparison group (Table 7).

Table 6: Canonical Pathways for 10 μg/mL vs. PBS.

Canonical Pathways	-log(p-value)	z-score	Proteins
Protein Synthesis-Related Pathway			
EIF2 Signaling	19.2	2.53	EIF1, EIF3C, EIF3D, EIF3L, EIF4A2, MAP2K1, PTBP1, RPL15, RPL18A, RPL19, RPL24, RPL30, RPL38, RPL5, RPL6, RPL7A, RPS11, RPS13, RPS17, RPS2, RPS21, RPS24, RPS26, RPS3, RPS4X, RPS4Y2, RPS8, RPS9, RPSA
Mitochondrial Related Pathway			
Oxidative Phosphorylation	4.39	1	MT-ATP6, NDUFA4, NDUFB5, NDUFB8, NDUFS1, NDUFS6, UQCRC1, UQCRC2, UQCRQ
Apoptosis-Related Pathways			
Apoptosis Signaling	3.27	-0.378	BAX, CASP7, CASP8, LMNA, MAP2K1, NFKBIB, RELA
Induction of Apoptosis by HIV1	2.73	-1.342	BAX, CASP8, FADD, NFKBIB, RELA
TNFR1 Signaling	3.17	-2.236	CASP7, CASP8, FADD, NFKBIB, RELA
Cell-Cell Adhesion-Related Pathways			
ILK Signaling	2.22	-1.342	DSP, GSK3A, ITGB4, KRT18, MTOR, RAC2, RELA, TMSB10/TMSB4X
Immune-Related Pathways			
Role of MAPK Signaling in Promoting the Pathogenesis of Influenza	1.68	-0.447	ATP6V1C1, BAX, MAP2K1, MAP2K3, NFKBIB
IL-6 Signaling	2.1	-0.816	IL36B, MAP2K1, MAP2K3, NFKBIB, RELA, TAB1
IL-1 Signaling	1.34	-1	MAP2K3, NFKBIB, RELA, TAB1
LPS-Stimulated MAPK Signaling	1.55	-1	MAP2K1, MAP2K3, NFKBIB, RELA
IL-15 Production	1.59	-1.342	CSK, MAP2K1, MAP2K3, PTK2B, RELA
IL-8 Signaling	2.04	-1.89	BAX, EIF4EBP1, MAP2K1, MTOR, NFKBIB, PTK2B, RAC2, RELA

Table 7: Canonical Pathways for 400 μg/mL vs. PBS.

Canonical Pathways	-log(p-value)	z-score	Proteins
Protein Synthesis-Related Pathway			
EIF2 Signaling	6.91	2	EIF1, EIF2B2, EIF2S2, EIF3M, EIF4A2, PTBP1, RPL18A, RPL38, RPS12, RPS15, RPS24, RPS26, RPS3, RPS4X, RRAS2
Immune-Related Pathways			
IL-1 Signaling	2.15	-0.447	MAP2K3, NFKBIB, PRKAR1A, RELA, TAB1
ERK/MAPK Signaling	2.29	-0.707	PAK1, PLA2G4A, PLA2G4D, PPP2R5A, PRKAR1A, PRKCI, PTK2B, RRAS2
MIF-Mediated Glucocorticoid Regulation	4.05	-1.342	MIF, NFKBIB, PLA2G4A, PLA2G4D, RELA
MIF Regulation of Innate Immunity	3.6	-1.342	MIF, NFKBIB, PLA2G4A, PLA2G4D, RELA
Cell-Cell Adhesion-Related Pathways			
Death Receptor Signaling	1.54	-1	ARHGDIB, CASP8, NFKBIB, RELA

IPA's regulator effect analysis for the Nic10 vs. PBS comparison produced the regulator effect network shown in Figure 7. This figure shows the four predicted upstream regulators and their connection to nine significantly altered proteins identified in our data. Those proteins were then linked to one downstream function, survival of organism, that was predicted to have been activated (Figure 5). The regulator effect analysis performed on the proteomics data collected from nicotine-treated EpiDerm^{TM} indicated that nicotine at a low dose activated survival pathways or a stress response without inducing cellular apoptosis or killing the cells. No regulator effects were identified for the Nic400 vs. PBS set.

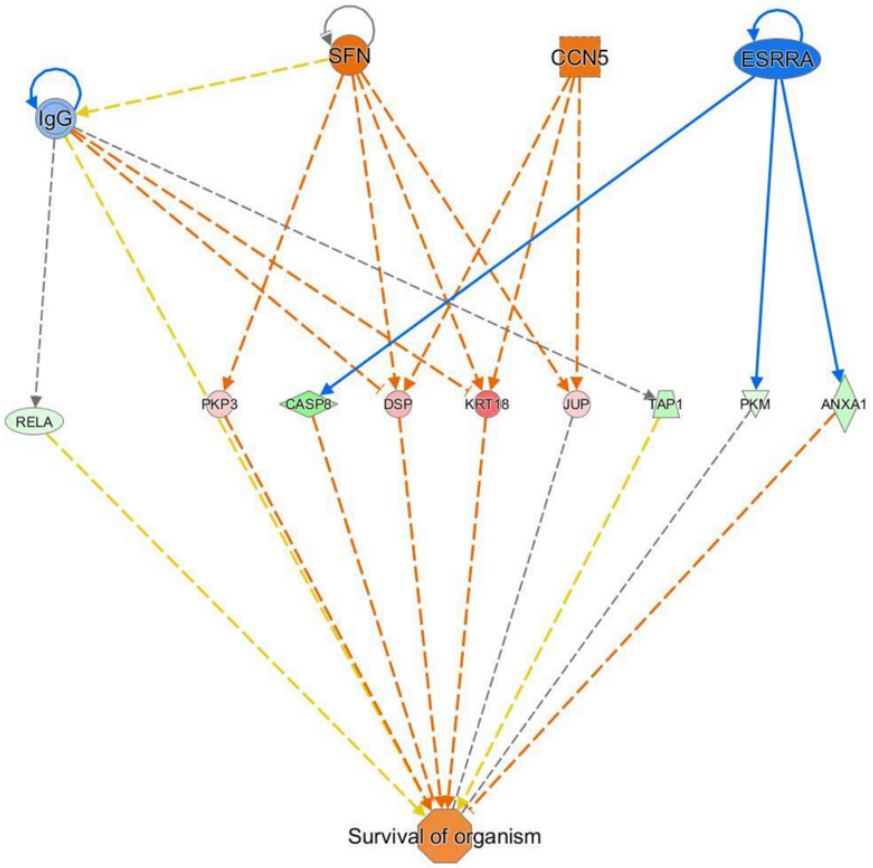

Figure 7: Regulator Effects diagram from 10 µg/mL vs. PBS group.

IPA was also used to perform toxicological analysis on the proteomics data extracted from nicotine-treated EpiDerm™ because nicotine is a chemical commonly associated with harmful effects. IPA-generated toxicity lists for Nic10 vs. PBS included terms related to mitochondrial dysfunction, oxidative stress response, cellular apoptosis, and gene regulation (Table 8). All proteins associated with "Pro-Apoptosis" were identified to have been downregulated, suggesting that nicotine treatment caused an anti-apoptotic effect (Table 8).

Toxicological analysis of proteomics data from the Nic400 vs. PBS set produced similar results to the Nic10 vs. PBS analysis. Much like the Nic10 vs. PBS analysis, the Nic400 vs. PBS analysis concluded that mitochondrial function, oxidative stress response, and gene regulation were affected (Table 9). Other terms that were observed in this higher-dose analysis included

PXR/RXR activation, hypoxia-inducible factor signaling, RAR activation, aryl hydrocarbon receptor signaling, cholesterol biosynthesis, and LXR/PXR activation (Table 9).

Table 8: IPA Toxicity List for 10 µg/mL of Nicotine vs. PBS.

IPA Toxicity Lists	-log(p-value)	Proteins*
Mitochondrial Dysfunction	5.41	CASP8, CPT1A, MT-ATP6, NDUFA4, NDUFB5, NDUFB8, NDUFS1, NDUFS6, PARK7, UQCRC1, UQCRC2, UQCRQ
NRF2-Mediated Oxidative Stress Response	2.27	AKR1A1, BACH1, DNAJB1, DNAJB11, DNAJB2, DNAJC11, DNAJC5, MAP2K1, MAP2K3
Decreased Respiration of Mitochondria	1.83	MFN1, PKM
Pro-Apoptosis	1.72	BAX, CASP7, CASP8
Increased Transmembrane Potential of Mitochondria and Mitochondrial Membrane	1.52	BAX, CASP7, DNAJB1
Mechanism of Gene Regulation by Peroxisome Proliferators via PPARα	1.4	MAP2K1, NFKBIB, RELA, TAB1

*Upregulated proteins are in red. Downregulated proteins are in blue.

Table 9: Toxicity Lists for 400 µg/mL of Nicotine vs. PBS.

IPA Toxicity Lists	-log(p-value)	Proteins*
Mitochondrial Dysfunction	4.34	CASP8, COX7A2, COX7C, NDUFA4, NDUFA8, NDUFA9, NDUFB5, NDUFS1, TXN2, UQCRQ
PXR/RXR Activation	2.95	GSTM2, PCK2, PRKAR1A, RELA, SCD
NRF2-Mediated Oxidative Stress Response	2.59	AKR1A1, BACH1, CDC34, DNAJC13, DNAJC5, GSTM2, MAP2K3, PRKCI, RRAS2
Mechanism of Gene Regulation by Peroxisome Proliferators via PPARα	2.23	FAT1, NFKBIB, PRKAR1A, RELA, TAB1
Decreases Depolarization of Mitochondria and Mitochondrial Membrane	2.07	PAK1, PLA2G4A, PPIA
Hypoxia-Inducible Factor Signaling	1.99	EIF1, EIF2B2, EIF2S2, UBE2N

RAR Activation	1.91	PRKAR1A, PRKCI, PRMT1, RDH12, RELA, SDR16C5, SMARCC2
Aryl Hydrocarbon Receptor Signaling	1.87	ALDH3A1, CDKN2A, CTSD, GSTM2, NEDD8, RELA
Cholesterol Biosynthesis	1.81	IDI1, SQLE
LXR/RXR Activation	1.77	ACACA, IL36B, PLTP, RELA, SCD
Oxidative Stress	1.5	GSTM2, RELA, S100A7

*Upregulated proteins are in red. Downregulated proteins are in blue.

7. DISCUSSION AND CONCLUSION

Both experiments described above aimed to investigate the effects that e-cigarettes and related chemicals have on the human body. Although e-cigarettes are commonly utilized for smoking cessation, they are not harm-free, especially when e-cigarette use continues after cessation of combustible cigarettes. The transcriptome-wide analysis of nasal epithelium from former smokers who switched to e-cigarettes addressed the harmfulness of e-cigarettes, especially when compared to non-smokers. Additionally, the use and handling of e-cigarettes puts individuals at risk for dermal exposure to nicotine, among other chemicals. Similarly, aged cigarette smoke, or THS, found in households and public indoor spaces puts people at risk for dermal nicotine exposure without being in close proximity of an active smoker. The proteomic analysis of human-derived EpiDerm^{TM} exposed to differing levels of nicotine identified and characterized the effects of dermal nicotine uptake.

Transcriptomic analysis of nasal epithelium biopsies in former cigarette smokers who had since converted to e-cigarettes for at least 6 months indicated that these individuals continued to present increased inflammatory and immune responses, and decreased formation of cilia when compared to those who had never used combustible cigarettes or e-cigarettes. In individuals who had ceased smoking combustible cigarettes for 14 days, inflammatory response biomarkers had been significantly reduced back towards non-smoker levels (Darabseh et al., 2021). Therefore,

we can conclude that continued e-cigarette use after smoking cessation was likely the cause of prolonged inflammation in our EC group. Specifically, degranulation of neutrophils was determined to be a significant response associated with an inflammatory reaction in former smokers who had switched to e-cigarettes. Degranulation of neutrophils, wherein primary and secondary granules are released to prevent tissue damage (Sengeløv et al., 1995), is one of the main mediators of lung and airway tissue damage, specifically associated with chronic obstructive pulmonary disease (COPD) (Hoenderdos & Condliffe, 2013). COPD is caused by cigarette smoking-related inflammation, and is known to cause progressive decline in lung function (Hoenderdos & Condliffe, 2013). Although COPD may persist after smoking cessation (Hoenderdos & Condliffe, 2013), symptoms of COPD tend to improve after quitting combustible cigarettes (Willemse et al., 2004). Therefore, the persistent inflammatory response caused by continued e-cigarette use in former smokers allows lung damage associated with neutrophil degranulation to continue, possibly leading to the onset or worsening of chronic lung diseases like COPD. Furthermore, e-cigarettes are known to contain pro-inflammatory chemicals, like propylene glycol, glycerol, and nicotine (Escobar et al., 2020, 2021). Our data on pro-inflammation agree with the conclusion that e-cigarette use in former smokers leads to persistent systemic and respiratory inflammation.

Both cigarette smoke and e-cigarette aerosol are detrimental to cilia health and ciliogenesis (Corbett et al., 2019; Tamashiro et al., 2009). Particularly, bronchial epithelium from former smokers who had converted to e-cigarettes exhibited the downregulation of genes that were indirectly linked to ciliogenesis (Corbett et al., 2019). Our transcriptomic analysis produced results which validate and provide further proof for this observed effect on the formation of cilia. Our data showed the downregulation of genes which are directly involved in ciliogenesis within

samples from individuals who also switched from combustible cigarettes to e-cigarettes. Our results are consistent with existing findings and further implicate that formation of cilia in respiratory tissues was negatively affected, not reversed, as a result of switching from combustible cigarettes to e-cigarettes.

Given the effect nicotine has when in contact with human skin via THS or e-liquid has not been well defined so far, this proteomics analysis is one of the first studies to address this topic. Analyzing protein expression changes of 3D human-derived EpiDerm™ in response to different levels of nicotine gave us insight to how nicotine may negatively affect human skin. These effects included an anti-inflammatory response leading to impaired would healing, an anti-apoptotic reaction, and altered mitochondria-related pathways.

Nicotine is known to have an anti-inflammatory effect in the skin (Zhang et al., 2022). The specific anti-inflammatory mechanism of nicotine is mediated by the α7 nicotinic acetylcholine receptors (nAChR) expressed in granular layers of human skin (Xanthoulea et al., 2013). As a result, nicotine has been used in case studies to treat certain inflammatory skin diseases like psoriasis with much success (Staples & Klein, 2012). However, this anti-inflammatory property also causes dermal nicotine exposure to delay wound healing (Xanthoulea et al., 2013). In a mouse model, it was shown that keratinocyte nAChR activation by nicotine led to the blocking of the NF-κB and Erk1/2 pathway, a known pathway involved in early and late wound healing, and toll-like receptor 2 (TLR2) signaling (Kishibe et al., 2015). Our data show immune and inflammatory inhibition as a result of nicotine exposure in a 3D human skin model. These findings were consistent with known effects of nicotine, and further demonstrated that specifically low-dose nicotine (Nic10) may be the main contributor to delayed would healing in certain experimental models.

Both experimental exposure levels of nicotine (Nic10 and Nic400) caused the proteomic analysis of EpiDerm™ to predict that EIF2 signaling pathway would be activated. The EIF2 signaling pathway, which is involved in global protein synthesis, encompasses the function of various proteins. Under toxic conditions, one of these proteins, eukaryotic translation initiation factor 2 alpha (eIF2α), may become phosphorylated (Liu & Qian, 2014). As a result, the eIF2α will selectively translate only a subset of mRNA, leading to a lack of encoded proteins necessary for cell survival and stress recovery (Liu & Qian, 2014). An effect of this restricted stress recovery is the inhibition of apoptosis, which should be triggered by stress (Szegezdi et al., 2006). Our data further support that the toxic environment caused by nicotine exposure at a low dose (Nic10) inhibited the EpiDerm™ model's response to stress and caused an observable anti-apoptotic effect as demonstrated by the downregulation of several apoptosis-related canonical pathways.

Mitochondrial dysfunction was identified in the IPA toxicity lists for both nicotine exposure levels (Nic10 and Nic400). Mitochondria are essential organelles for maintaining proper cellular function and biological processes through the production of ATP. Additionally, mitochondria produce reactive oxygen species (ROS) and are themselves susceptible to oxidative injury leading to mitochondrial dysfunction (Meng et al., 2021). In a positive-feedback loop that leads to chronic oxidative damage, the ROS-induced mitochondrial dysfunction causes increased ROS production (Meng et al., 2021). Previous studies have shown that nicotine caused ROS accumulation and impaired proper mitochondrial function and autophagy (Wang et al., 2020). IPA canonical pathway analysis also demonstrated that nicotine exposure in both the Nic10 and Nic400 experimental groups caused NFR2-mediated stress response. In the lower dose exposure of Nic10, an additional canonical pathway, oxidative phosphorylation, was increased. In the

higher dose exposure of Nic400, oxidative stress was also identified as an affected toxicity list. Our data support the conclusion that dermal exposure to nicotine caused increased oxidative stress response, leading to ROS increased production by mitochondria and subsequent damage to mitochondrial function.

Although both previously described ‘omics analyses produced significant and substantial results, there were certain experimental factors and limitations that should be considered. In the transcriptomic analysis of the effects of switching from combustible cigarettes to e-cigarettes, the cigarette user group contained three participants with highly variable cigarette-use patterns, as displayed in Table 1. Along those lines, the CS vs. NS comparison group produced far fewer DEGs than the EC vs. NS comparison group. This discrepancy in identified DEGs between the two groups may have been caused by the variability in cigarette exposure, and might explain why fewer significant pathways were characterized. In future studies, larger, more consistent samples should be utilized to address this issue. The proteomic analysis of EpiDerm^{TM} and related experimentation did not have any significant confounding factors.

In conclusion, our data support existing knowledge that switching from cigarettes to e-cigarettes for at least 6 months does not reverse the damaging effects of cigarette use. Furthermore, transcriptomic analysis of nasal epithelium from former smokers who converted to e-cigarettes suggested an increased inflammatory and immune response and inhibited formation of cilia. Although it is difficult to know whether the differences observed in the experimental group was due to past cigarette use, current e-cigarette use, or a combination of the two, our data show significant evidence of the damage e-cigarette use may cause after smoking cessation. Additionally, both low and high dose dermal exposure to nicotine using a 3D human skin model significantly affected many biological pathways and functions. Proteomic analysis suggested an

anti-inflammatory response which could impair wound healing, an anti-apoptotic response, and mitochondrial dysfunction. It was determined that even a low dose exposure to nicotine was able to significantly alter the EpiDerm^{TM} proteome. Together, results from these 'omic analyses indicate that the safety of e-cigarettes as a replacement for cigarettes must be further researched. The use of nicotine has detrimental health effects, whether the exposure is by inhalation or by dermal contact. Further investigation is needed to better understand the effects of nicotine in general, and specifically in THS and e-cigarettes to inform potential public health measures to combat smoke and e-cigarette aerosol exposure.

8. ABSTRACT REFERENCES

Pozuelos, G., **Rubin, M.A.,** Vargas, S., Ramirez, E., Bandaru, D., Talbot, P. (In Review). *Nicotine affects multiple biological processes in EpiDerm organotypic tissues and keratinocyte monolayers.* Atmosphere.

Pozuelos, G., Kagda, M., **Rubin, M.A.**, Goniewicz, M.L., Girke, T., Talbot, P. (In Review). *Transcriptomic evidence that switching from tobacco to electronic cigarette does not reverse damage to the respiratory epithelium*. Toxics.

9. REFERENCES

Bahl, V., Shim, H. J., Jacob, P., Dias, K., Schick, S. F., & Talbot, P. (2016). Thirdhand smoke: Chemical dynamics, cytotoxicity, and genotoxicity in outdoor and indoor environments. *Toxicology in Vitro: An International Journal Published in Association with BIBRA*, *32*, 220–231. https://doi.org/10.1016/j.tiv.2015.12.007

Behar, R. Z., Wang, Y., & Talbot, P. (2018). Comparing the cytotoxicity of electronic cigarette fluids, aerosols and solvents. *Tobacco Control*, *27*(3), 325–333. https://doi.org/10.1136/tobaccocontrol-2016-053472

Canistro, D., Vivarelli, F., Cirillo, S., Babot Marquillas, C., Buschini, A., Lazzaretti, M., Marchi, L., Cardenia, V., Rodriguez-Estrada, M. T., Lodovici, M., Cipriani, C., Lorenzini, A., Croco, E., Marchionni, S., Franchi, P., Lucarini, M., Longo, V., Della Croce, C. M., Vornoli, A., … Paolini, M. (2017). E-cigarettes induce toxicological effects that can raise the cancer risk. *Scientific Reports*, *7*(1), 2028. https://doi.org/10.1038/s41598-017-02317-8

CDC. (2020, January 23). *Adult Smoking Cessation—The Use of E-Cigarettes*. https://www.cdc.gov/tobacco/data_statistics/sgr/2020-smoking-cessation/fact-sheets/adult-smoking-cessation-e-cigarettes-use/index.html

CDCTobaccoFree. (2022, March 17). *Data and Statistics*. Centers for Disease Control and Prevention. https://www.cdc.gov/tobacco/data_statistics/index.htm

Corbett, S. E., Nitzberg, M., Moses, E., Kleerup, E., Wang, T., Perdomo, C., Perdomo, C., Liu, G., Xiao, X., Liu, H., Elashoff, D. A., Brooks, D. R., O'Connor, G. T., Dubinett, S. M., Spira, A., & Lenburg, M. E. (2019). Gene Expression Alterations in the Bronchial

Epithelium of e-Cigarette Users. *Chest*, *156*(4), 764–773. https://doi.org/10.1016/j.chest.2019.05.022

Darabseh, M. Z., Maden-Wilkinson, T. M., Welbourne, G., Wüst, R. C. I., Ahmed, N., Aushah, H., Selfe, J., Morse, C. I., & Degens, H. (2021). Fourteen days of smoking cessation improves muscle fatigue resistance and reverses markers of systemic inflammation. *Scientific Reports*, *11*(1), 12286. https://doi.org/10.1038/s41598-021-91510-x

Davis, B., Dang, M., Kim, J., & Talbot, P. (2015). Nicotine Concentrations in Electronic Cigarette Refill and Do-It-Yourself Fluids. *Nicotine & Tobacco Research*, *17*(2), 134–141. https://doi.org/10.1093/ntr/ntu080

Draghici, S., Khatri, P., Tarca, A. L., Amin, K., Done, A., Voichita, C., Georgescu, C., & Romero, R. (2007). A systems biology approach for pathway level analysis. *Genome Research*, *17*(10), 1537–1545. https://doi.org/10.1101/gr.6202607

Escobar, Y.-N. H., Morrison, C. B., Chen, Y., Hickman, E., Love, C. A., Rebuli, M. E., Surratt, J. D., Ehre, C., & Jaspers, I. (2021). Differential responses to e-cig generated aerosols from humectants and different forms of nicotine in epithelial cells from nonsmokers and smokers. *American Journal of Physiology. Lung Cellular and Molecular Physiology*, *320*(6), L1064–L1073. https://doi.org/10.1152/ajplung.00525.2020

Escobar, Y.-N. H., Nipp, G., Cui, T., Petters, S. S., Surratt, J. D., & Jaspers, I. (2020). In Vitro Toxicity and Chemical Characterization of Aerosol Derived from Electronic Cigarette Humectants Using a Newly Developed Exposure System. *Chemical Research in Toxicology*, *33*(7), 1677–1688. https://doi.org/10.1021/acs.chemrestox.9b00490

Garcia, R., Allem, J. P., Baezconde-Garbanati, L., Unger, J. B., & Sussman, S. (2016). Employee and customer handling of nicotine-containing e-liquids in vape shops. *Tobacco Prevention & Cessation*, *2*(Suppl), 10.18332/tpc/67295.

Health, C. O. on S. and. (2020, November 16). *Smoking and Tobacco Use; Electronic Cigarettes*. Centers for Disease Control and Prevention. https://www.cdc.gov/tobacco/basic_information/e-cigarettes/about-e-cigarettes.html

Hoenderdos, K., & Condliffe, A. (2013). The neutrophil in chronic obstructive pulmonary disease. *American Journal of Respiratory Cell and Molecular Biology*, *48*(5), 531–539. https://doi.org/10.1165/rcmb.2012-0492TR

Hughes, J. R. (2003). Motivating and Helping Smokers to Stop Smoking. *Journal of General Internal Medicine*, *18*(12), 1053–1057. https://doi.org/10.1111/j.1525-1497.2003.20640.x

Jacob, P., Benowitz, N. L., Destaillats, H., Gundel, L., Hang, B., Martins-Green, M., Matt, G. E., Quintana, P. J. E., Samet, J. M., Schick, S. F., Talbot, P., Aquilina, N. J., Hovell, M. F., Mao, J.-H., & Whitehead, T. P. (2017). Thirdhand Smoke: New Evidence, Challenges, and Future Directions. *Chemical Research in Toxicology*, *30*(1), 270–294. https://doi.org/10.1021/acs.chemrestox.6b00343

Kalkhoran, S., & Glantz, S. A. (2016). E-cigarettes and smoking cessation in real-world and clinical settings: A systematic review and meta-analysis. *The Lancet. Respiratory Medicine*, *4*(2), 116–128. https://doi.org/10.1016/S2213-2600(15)00521-4

Khachatoorian, C., Jacob III, P., Benowitz, N. L., & Talbot, P. (2019). Electronic cigarette chemicals transfer from a vape shop to a nearby business in a multiple-tenant retail building. *Tobacco Control*, *28*(5), 519–525. https://doi.org/10.1136/tobaccocontrol-2018-054316

Kishibe, M., Griffin, T. M., & Radek, K. A. (2015). Keratinocyte nicotinic acetylcholine receptor activation modulates early TLR2-mediated wound healing responses. *International Immunopharmacology*, *29*(1), 63–70. https://doi.org/10.1016/j.intimp.2015.05.047

Krämer, A., Green, J., Pollard, J., & Tugendreich, S. (2014). Causal analysis approaches in Ingenuity Pathway Analysis. *Bioinformatics (Oxford, England)*, *30*(4), 523–530. https://doi.org/10.1093/bioinformatics/btt703

Liu, B., & Qian, S.-B. (2014). Translational reprogramming in cellular stress response. *WIREs RNA*, *5*(3), 301–305. https://doi.org/10.1002/wrna.1212

Matt, G. E., Quintana, P. J. E., Hovell, M. F., Bernert, J. T., Song, S., Novianti, N., Juarez, T., Floro, J., Gehrman, C., Garcia, M., & Larson, S. (2004). Households contaminated by environmental tobacco smoke: Sources of infant exposures. *Tobacco Control*, *13*(1), 29–37. https://doi.org/10.1136/tc.2003.003889

Matt, G. E., Quintana, P. J. E., Zakarian, J. M., Fortmann, A. L., Chatfield, D. A., Hoh, E., Uribe, A. M., & Hovell, M. F. (2011). When smokers move out and non-smokers move in: Residential thirdhand smoke pollution and exposure. *Tobacco Control*, *20*(1), e1–e1. https://doi.org/10.1136/tc.2010.037382

McAlinden, K. D., Eapen, M. S., Lu, W., Sharma, P., & Sohal, S. S. (2020). The rise of electronic nicotine delivery systems and the emergence of electronic-cigarette-driven disease. *American Journal of Physiology-Lung Cellular and Molecular Physiology*, *319*(4), L585–L595. https://doi.org/10.1152/ajplung.00160.2020

McKnight, R. H., & Spiller, H. A. (2005). Green Tobacco Sickness in Children and Adolescents. *Public Health Reports*, *120*(6), 602–605. https://doi.org/10.1177/003335490512000607

Meng, T., Wang, W., Meng, F., Wang, S., Wu, H., Chen, J., Zheng, Y., Wang, G., Zhang, M., Li, Y., & Su, G. (2021). Nicotine Causes Mitochondrial Dynamics Imbalance and Apoptosis Through ROS Mediated Mitophagy Impairment in Cardiomyocytes. *Frontiers in Physiology*, *12*. https://www.frontiersin.org/article/10.3389/fphys.2021.650055

Pozuelos, G. L., Jacob, P., Schick, S. F., Omaiye, E. E., & Talbot, P. (2021). Adhesion and Removal of Thirdhand Smoke from Indoor Fabrics: A Method for Rapid Assessment and Identification of Chemical Repositories. *International Journal of Environmental Research and Public Health*, *18*(7), 3592. https://doi.org/10.3390/ijerph18073592

Salzman, G. A., Alqawasma, M., & Asad, H. (2019). Vaping Associated Lung Injury (EVALI): An Explosive United States Epidemic. *Missouri Medicine*, *116*(6), 492–496.

Sengeløv, H., Follin, P., Kjeldsen, L., Lollike, K., Dahlgren, C., & Borregaard, N. (1995). Mobilization of granules and secretory vesicles during in vivo exudation of human neutrophils. *Journal of Immunology (Baltimore, Md.: 1950)*, *154*(8), 4157–4165.

Singh, A., Pandey, P., Tewari, M., Pandey, H., Gambhir, I., & Shukla, H. (2016). Free radicals hasten head and neck cancer risk: A study of total oxidant, total antioxidant, DNA damage, and histological grade. *Journal of Postgraduate Medicine*, *62*(2), 96–101. https://doi.org/10.4103/0022-3859.180555

Sleiman, M., Gundel, L. A., Pankow, J. F., Jacob, P., Singer, B. C., & Destaillats, H. (2010). Formation of carcinogens indoors by surface-mediated reactions of nicotine with nitrous acid, leading to potential thirdhand smoke hazards. *Proceedings of the National Academy of Sciences of the United States of America*, *107*(15), 6576–6581. https://doi.org/10.1073/pnas.0912820107

Staples, J., & Klein, D. (2012). Can nicotine use alleviate symptoms of psoriasis? *Canadian Family Physician Médecin de Famille Canadien*, *58*, 404–408.

Subramanian, I., Verma, S., Kumar, S., Jere, A., & Anamika, K. (2020). Multi-omics Data Integration, Interpretation, and Its Application. *Bioinformatics and Biology Insights*, *14*. https://doi.org/10.1177/1177932219899051

Szegezdi, E., Logue, S. E., Gorman, A. M., & Samali, A. (2006). Mediators of endoplasmic reticulum stress-induced apoptosis. *EMBO Reports*, *7*(9), 880–885. https://doi.org/10.1038/sj.embor.7400779

Tamashiro, E., Xiong, G., Anselmo-Lima, W. T., Kreindler, J. L., Palmer, J. N., & Cohen, N. A. (2009). Cigarette smoke exposure impairs respiratory epithelial ciliogenesis. *American Journal of Rhinology & Allergy*, *23*(2), 117–122. https://doi.org/10.2500/ajra.2009.23.3280

Teriba, A., Mbama, U., Sharma, S., Abraham, A., & Ndefo, U. A. (2021). Evidence against e-cigarettes for smoking cessation. *Journal of the American Pharmacists Association*, *61*(5), e55–e58. https://doi.org/10.1016/j.japh.2021.05.001

Wang, S.-Y., Ni, X., Hu, K.-Q., Meng, F.-L., Li, M., Ma, X.-L., Meng, T.-T., Wu, H.-H., Ge, D., Zhao, J., Li, Y., & Su, G.-H. (2020). Cilostazol alleviate nicotine induced cardiomyocytes hypertrophy through modulation of autophagy by CTSB/ROS/p38MAPK/JNK feedback loop. *International Journal of Biological Sciences*, *16*(11), 2001–2013. https://doi.org/10.7150/ijbs.43825

Willemse, B. W. M., Postma, D. S., Timens, W., & Hacken, N. H. T. ten. (2004). The impact of smoking cessation on respiratory symptoms, lung function, airway hyperresponsiveness

and inflammation. *European Respiratory Journal*, *23*(3), 464–476. https://doi.org/10.1183/09031936.04.00012704

Xanthoulea, S., Deliaert, A., Romano, A., Rensen, S. S., Buurman, W. A., & van der Hulst, R. R. (2013). Nicotine effect on inflammatory and growth factor responses in murine cutaneous wound healing. *International Immunopharmacology*, *17*(4), 1155–1164. https://doi.org/10.1016/j.intimp.2013.10.022

Yu, G., Wang, L.-G., Yan, G.-R., & He, Q.-Y. (2015). DOSE: An R/Bioconductor package for disease ontology semantic and enrichment analysis. *Bioinformatics*, *31*(4), 608–609. https://doi.org/10.1093/bioinformatics/btu684

Zhang, W., Lin, H., Zou, M., Yuan, Q., Huang, Z., Pan, X., & Zhang, W. (2022). Nicotine in Inflammatory Diseases: Anti-Inflammatory and Pro-Inflammatory Effects. *Frontiers in Immunology*, *13*. https://www.frontiersin.org/article/10.3389/fimmu.2022.826889